Adaptive $\mathcal{U}_L$-Coded Spectrally-Precoded OFDM With Zero-Forcing Equalization Under Flat Fading

Wei-Lun Lin*, Yan-Ru Peng†, and Char-Dir Chung‡
* Graduate Institute of Communication Engineering, National Taiwan University, Taipei 10617 Taiwan
E-mail: weilunlin@ntu.edu.tw Tel/Fax: +886-2-3366-3596
†Institute for Information Industry, Taipei 10617 Taiwan
E-mail: rethy@nmi.iii.org.tw Tel: +886-2-2987-3109
‡Department of Electrical Engineering and Graduate Institute of Communication Engineering,
National Taiwan University, Taipei 10617 Taiwan
E-mail: cdchung@cc.ee.ntu.edu.tw Tel/Fax: +886-2-3366-3596

***Abstract*—Constant-power adaptive transmission technique adopting $\mathcal{U}_L$-coded spectrally-precoded orthogonal frequency-division multiplexing (SP-OFDM) signals with one tap zero-forcing equalization is studied on the flat fading channel. By jointly adapting the precoding order for spectral precoder and the component modulation for OFDM, constant-power $\mathcal{U}_L$-coded adaptive SP-OFDM is shown to outperform conventional constant-power adaptive OFDM significantly in average spectral efficiency.**[1]

I. Introduction

Typically, orthogonal frequency division multiplexing (OFDM) systems shape the transmitted signal with the rectangular pulse for efficient implementation of discrete Fourier transform (DFT) and the insertion of guard intervals to counteract channel dispersion, which results in large power spectral sidelobes decaying asymptotically as f^{-2} [1]-[4]. In order to prevent excessive interference to adjacent channels, redundant guard bands [5] and transmitter filtering [6] are commonly employed in practical applications at the cost of spectral and power efficiencies. Recently, several spectral precoding schemes [1]-[4] are proposed to improve the spectral compactness of the rectangularly-pulsed OFDM signals. These spectrally-precoded OFDM (SP-OFDM) signals, can not only facilitate the standard DFT-based OFDM implementation and the insertion of cyclic prefix (CP) or zero padding (ZP) in the guard intervals to counteract channel dispersion, but also provide very small power spectral sidelobes. In [4], much higher spectral compactness, and thus much higher spectral efficiency, than the spectrally uncoded OFDM signal can be achieved for the $\mathcal{G}_L$-coded SP-OFDM signal with ZP and $\mathcal{U}_L$-coded SP-OFDM signal with CP or ZP with power spectral sidelobes decaying asymptotically as f^{-2L-2}, especially when the precoding order L is large. Besides, $\mathcal{U}_L$-coded SP-OFDM is found to provide the system error performance comparable to spectrally uncoded OFDM on the additive white Gaussian noise (AWGN) channel and the multipath fading channels, though $\mathcal{G}_L$-coded SP-OFDM outperforms spectrally uncoded OFDM only on severely faded multipath channels.

Since the precoding order L can be increased to provide higher spectral efficiency, SP-OFDM is suited for adaptive transmission to pursue higher system throughput. By jointly adapting the precoding order L and the constellation size K of quadrature amplitude modulation (QAM) according to the estimated channel status under a preassigned bit error rate (BER), the $\mathcal{G}_L$-coded adaptive SP-OFDM (ASP-OFDM) system in [7] is shown to significantly outperform the conventional adaptive OFDM system [5], [8]-[10] in average spectral efficiency. However, considerable computation effort is required for the block decoding of the correlatively encoded $\mathcal{G}_L$-coded SP-OFDM signals [1], [7], whereas the $\mathcal{U}_L$-coded SP-OFDM signal can be easily recovered through one tap zero-forcing equalization owning to the orthogonality being maintained between the subcarriers of the $\mathcal{U}_L$-coded SP-OFDM signal. Based on the simple receiver structure for the ease of implementation, $\mathcal{U}_L$-coded SP-OFDM is considered in this paper to combine adaptive modulation with an attempt to provide higher system throughput than adaptive OFDM.

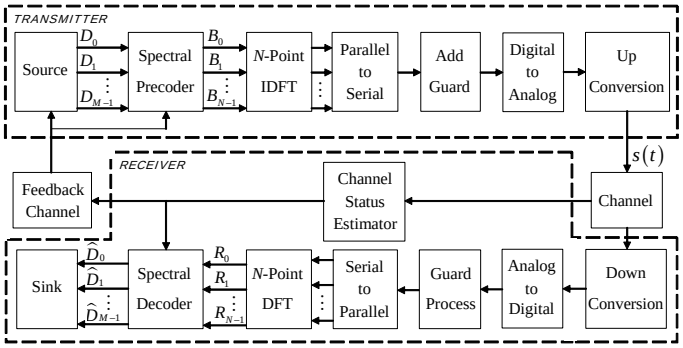

Fig. 1. The ASP-OFDM system model.

II. System Model

Fig. 1 depicts the $2N$-dimensional ($2N$-D) ASP-OFDM system. Denote $T = T_d + T_g$ as the length of the block time interval for transmitting a block of M data symbols, where T_d and T_g are the lengths for the useful data subinterval

[1]This work was supported by the ROC National Science Council under Contract 97-2221-E-002-011-MY3.

and the guard subinterval, respectively, and $N > M$ is assumed. Specifically, in a nominal block interval, the source generates a block of M independent and memoryless K-ary QAM symbols $\{D_m | m \in \mathcal{Z}_M\}$ with zero mean and unit variance, where $\mathcal{Z}_I \triangleq \{0, 1, ..., I-1\}$. These M symbols $\{D_m | m \in \mathcal{Z}_M\}$ are then spectrally precoded to yield a block of N transmitted complex symbols $\{B_n | n \in \mathcal{Z}_N\}$ as

$$B_n = \sum_{m=0}^{M-1} G_{n,m} D_m,\ n \in \mathcal{Z}_N. \tag{1}$$

With $L \triangleq N - M$ denoting the precoding order, the complex-valued precoding coefficient $G_{n,m}$ is defined by

$$G_{n,m} = \begin{cases} \mu_{n,m}, & 0 \le n-m \le L \\ 0, & \text{otherwise} \end{cases} \tag{2}$$

for $\mathcal{G}_L$ code [1], where $\mu_{n,m} = \binom{2L}{L}^{-1/2} \binom{L}{n-m} \zeta_n$ with $\omega_d \triangleq 2\pi/T_d$ and $\zeta_n = \exp\{-j\omega_d T_g n/2\}$ for SP-OFDM with CP and $\zeta_n = 1$ for SP-OFDM with ZP, and

$$\underline{G}_m = \frac{\underline{w}_m}{\|\underline{w}_m\|},\ m \in \mathcal{Z}_M \tag{3}$$

for $\mathcal{U}_L$ code [4], where $\underline{G}_m \triangleq [G_{0,m}, G_{1,m}, ..., G_{N-1,m}]^t$ and $\underline{w}_m \triangleq [w_{0,m}, w_{1,m}, ..., w_{N-1,m}]^t$ is obtained via the Gram-Schmidt recursion $\underline{w}_m = \underline{\mu}_m - \sum_{l=0}^{m-1} (\underline{w}_m^t \underline{\mu}_l / \|\underline{w}_l\|^2) \underline{w}_l$ with $\underline{\mu}_m \triangleq [\mu_{0,m}, \mu_{1,m}, ..., \mu_{N-1,m}]^t$ and $\underline{w}_0 = \underline{\mu}_0$.[2]

By monitoring the channel status, i.e., the instantaneously received signal-to-noise power ratio (SNR) γ, fed back from the receiver, both source and spectral precoder operate adaptively so that an SP-OFDM component modulation with appropriately chosen parameters L (the precoding order) and K (the modulation size) is used for transmission. Note that the SP-OFDM component modulation signals with larger L or K can provide higher spectral efficiency when the required out-of-band power fraction is extremely small. This property is to be explored in the design of the ASP-OFDM system.

After the precoder, $\{B_n | n \in \mathcal{Z}_N\}$ are modulated in parallel with N subcarriers, uniformly spaced by ω_d, and multiplexed to form the transmitted ASP-OFDM signal [1]-[4], [7] as

$$s(t) = \sqrt{S}\,\mathrm{Re}\left\{ \sum_{n=0}^{N-1} B_n \exp\{j(\omega_0 + n\omega_d)t\} \right\} \tag{4}$$

in the useful data subinterval $-T_d/2 \le t < T_d/2$, where S represents the instantaneous power and ω_0 is the reference frequency with $\omega_0 \gg \omega_d$. In the guard subinterval $-T_g - T_d/2 \le t < -T_d/2$, the transmitted signal is given by $s(t) = s(t+T_d)$ for ASP-OFDM with CP and $s(t) = 0$ for ASP-OFDM with ZP. Note that $s(t)$ can be generated from $\{B_n | n \in \mathcal{Z}_N\}$ by a standard inverse discrete Fourier transform (IDFT) -based OFDM process as in Fig. 1.

In this paper, ASP-OFDM with a small N (the number of subcarriers) is considered for design and performance in flat fading channels. Although not treated explicitly, the results can also be applied to ASP-OFDM with a large number of subcarriers in the frequency-selective fading channel wherein the total band is modeled as a partition of subbands in a way that all subcarriers in a subband suffer the same fade. This subband flat fading model is plausible when the coherence bandwidth of the frequency-selective fading channel exceeds the bandwidth of a subband and commonly assumed for the study in AOFDM systems [8]-[9].

Assume that the received signal is perfectly synchronized in amplitude, phase, symbol timing, and frequency by the DFT-based receiver in Fig. 1. The received waveform is down-converted, digitally sampled, and then manipulated block by block by the guard process. The guard process extracts useful samples for data detection by overlapping and adding the guard samples to the useful data samples for ASP-OFDM with ZP and by simply removing the guard samples for ASP-OFDM with CP [4]. After the guard process, the output samples are transformed by DFT to yield $\{R_n | n \in \mathcal{Z}_N\}$ where R_n represents the received complex symbol on the n-th subcarrier. Assuming that the guard subinterval is long enough to reject the inter-symbol interference, R_n can be modeled by $R_n = \sqrt{S} H B_n + W_n$ where H is the flat fading amplitude that is assumed to remain constant within the nominal block interval and $\{W_n | n \in \mathcal{Z}_N\}$ are the identically-distributed circularly-symmetric complex AWGN samples with mean zero and variance $E\{|W_n|^2\} = N_0$. For ASP-OFDM with CP, W_n's are mutually independent. For ASP-OFDM with ZP and $T_g = JT_d/N$, W_n's are correlated with $E\{W_n W_m^*\} = N_0 \sigma_{n-m}$ for $n \ne m$ where $\sigma_k = \frac{1}{N+J} \sum_{l=0}^{J-1} \exp\{-j\frac{2\pi}{N} lk\}$ with J being the number of zero-padded symbols in each guard subinterval.

By monitoring $\{R_n | n \in \mathcal{Z}_N\}$, the channel status estimator estimates the fading amplitude H and the received SNR γ, and passes the estimate for H to the spectral decoder and the estimate for γ to the transmitter through a feedback channel, respectively. It is assumed that H and γ are perfectly measured and the estimate for γ is fedback to the transmitter without error nor delay. Using the estimate for H, the symbol decisions $\{\widehat{D}_m = \widehat{D}_m^{(I)} + j\widehat{D}_m^{(Q)} | m \in \mathcal{Z}_M\}$ can be obtained by the spectral decoder through applying the block decoding rule [4] on $\{R_n = R_n^{(I)} + jR_n^{(Q)} | n \in \mathcal{Z}_N\}$ for the $\mathcal{G}_L$-coded SP-OFDM component modulation as

$$\begin{aligned} \left\{ \widehat{D}_m^{(x)} | m \in \mathcal{Z}_M \right\} \;=\; & \arg \left\{ \min_{\{D_m^{(x)} | m \in \mathcal{Z}_M\}} \sum_{n=0}^{N-1} \left| R_n^{(x)} \right. \right. \\ & -\sqrt{S} H \sum_{m=\max\{0,n-L\}}^{\min\{M-1,n\}} \binom{2L}{L}^{-\frac{1}{2}} \\ & \left. \left. \cdot \binom{L}{n-m} D_m^{(x)} \right|^2 \right\} \end{aligned} \tag{5}$$

with $D_m = D_m^{(I)} + jD_m^{(Q)}$ and $x = I$ and Q, and applying the zero-forcing symbol decoding rule [4] for the $\mathcal{U}_L$-coded

[2] $\underline{x}^t$ and $\|\underline{x}\|$ denote the transpose and the Frobenius norm, respectively, of $\underline{x}$.

SP-OFDM component modulation as

$$\widehat{D}_m = \arg\left\{ \min_{D_m} \left| D_m - \sum_{n=0}^{N-1} G_{n,m}^{*} \frac{R_n}{\sqrt{S}H} \right|^2 \right\}, \text{ for } m \in \mathcal{Z}_M. \tag{6}$$

For a nominal block interval containing M K-ary QAM symbols, the decoding algorithms in (5) for $\mathcal{G}_L$-coded SP-OFDM and in (6) for $\mathcal{U}_L$-coded SP-OFDM require $2K^M(2N-1)$ real additions and $6K^MN$ real multiplications, and $MK(4N+1)$ real additions and $4MK(N+1)$ real multiplications, respectively.[3] Obviously, the $\mathcal{U}_L$-coded SP-OFDM signal is much easier to be decoded than the $\mathcal{G}_L$-coded SP-OFDM signal, especially when K or M is large.

III. Adaptation Scheme

We consider the constant-power adaptation scheme with the instantaneous BER constrained by a target BER, i.e., BER_T, as developed in [10]. The constant-power adaptation scheme fixes the transmission power and is simple to implement, however, at the cost of marginally reduced average spectral efficiency comparing to the variable-power adaptation [9]-[10].

For adapting an SP-OFDM component modulation, the received SNR region is partitioned into $V+1$ subregions in a way that the v-th SP-OFDM component modulation λ_v is chosen for transmission when $\gamma \in [\Upsilon_{\lambda_v}, \Upsilon_{\lambda_{v+1}})$ with $v \in \mathcal{Z}_V$ where Υ_{λ_v} denotes the v-th modulation-switching threshold, and that no signal is transmitted when $\gamma < \Upsilon_{\lambda_0}$, and we set $\Upsilon_{\lambda_V} \triangleq \infty$ by default. Specifically, the adaptation criterion maximizes the average spectral efficiency η as

$$\eta = \sum_{v=0}^{V-1} \Phi_{\lambda_v} \left[F_\gamma\left(\Upsilon_{\lambda_{v+1}}\right) - F_\gamma\left(\Upsilon_{\lambda_v}\right) \right] \quad \text{bits/sec/Hz} \tag{7}$$

under the constraints that the average transmission power satisfies

$$\int_{\Upsilon_{\lambda_0}}^{\infty} Sp\left(\gamma\right) d\gamma = 1 \tag{8}$$

and that the instantaneous BER is not larger than BER_T as

$$BER_{\lambda_v}\left(\gamma\right) \le BER_T,\ v \in \mathcal{Z}_V. \tag{9}$$

Here, $BER_{\lambda_v}\left(\gamma\right)$ is the BER function when adopting λ_v. Φ_{λ_v} is the the spectral efficiency defined by the inverse of the normalized bandwidth $\left(CT_b\right)^{-1}$ required to capture a preassigned fraction $\wp$ of total power within a bandwidth C, with T_b being the bit time. $p\left(\cdot\right)$ and $F_\gamma\left(\cdot\right)$ are the probability density function and the cumulative distribution function of γ, respectively. In this paper, H is assumed to follow Rayleigh statistic [8] and in this case

$$F_\gamma\left(\Upsilon_{\lambda_v}\right) = 1 - \exp\left(-\Upsilon_{\lambda_v}/\overline{\gamma}\right) \tag{10}$$

with $\overline{\gamma}$ denoting the average SNR. It should be noted that (10) can be easily generalized to other amplitude fading statistics.

[3]The computation $\sum_{m=\max\{0,n-L\}}^{\min\{M-1,n\}} \binom{2L}{L}^{-1/2} \binom{L}{n-m} D_m^{(x)}$ for $n \in \mathcal{Z}_N$ is assumed prestored and not counted in the real additions and real multiplications.

The optimum solution of $\{\Upsilon_{\lambda_v} | v \in \mathcal{Z}_V\}$ and the instantaneous transmission power for ASP-OFDM has been provided in [10] as

$$\Upsilon_{\lambda_v} = \Gamma_{\lambda_v}\left[1 - F_\gamma\left(\Gamma_{\lambda_0}\right)\right] \text{ for } v \in \mathcal{Z}_V \tag{11}$$

and

$$S = \int_{\Upsilon_{\lambda_0}}^{\infty} p\left(\gamma\right) d\gamma, \tag{12}$$

where Γ_{λ_v} is the power efficiency defined by the SNR value required to achieve BER_T when adopting λ_v.

Denote $\Lambda \triangleq \{\lambda_v | v \in \mathcal{Z}_V\}$ as the set of $2N$-D SP-OFDM component modulations which is obtained from the modulation set Θ containing all $2N$-D SP-OFDM modulations with $L \in \{1, 2, ..., L_{\max}\}$ and $K \in \{4, 16, ..., K_{\max}\}$. Given the preassigned system design values BER_T and $\wp$, the following rule [7] is adopted to choose the component modulations in Λ from Θ: First, the most spectrally efficient modulation in Θ is chosen as λ_{V-1}. Second, when λ_{V-1}, λ_{V-2},...,λ_{V-m-1} are determined, λ_{V-m-2} is chosen as the modulation giving the highest spectral efficiency among all the modulations in Θ which are more power-efficient than λ_{V-m-1}. The second step is recursively repeated for $m \in \mathcal{Z}_{V-1}$ until $m = V-2$ or Θ is exhausted. As an example, Table I lists Λ's obtained from Θ with $L_{\max} = 3$ and $K_{\max} = 64$ when $N = 8$, $T_g = T_d/8$, $BER_T = 10^{-3}$, and $\wp = 0.99$ and 0.999. When $\wp = 0.99$, most chosen component modulations are shown to have $L = 1$ in that $\mathcal{G}_1$-coded SP-OFDM scheme provides sufficiently high spectral efficiency while yielding the largest possible power efficiency among all $\mathcal{G}_L$-coded SP-OFDM schemes. However, such a performance phenomenon vanishes when a higher value $\wp = 0.999$ is required.

IV. Numerical Results

Figs. 2 and 3 show the average spectral efficiency characteristics among the $\mathcal{G}_L$ and $\mathcal{U}_L$ -coded ASP-OFDM schemes and adaptive OFDM under flat Rayleigh fading when $N = 8$, $T_g = T_d/8$, $BER_T = 10^{-3}$, and $\wp = 0.99$ and 0.999, where the modulation sets Λ's are chosen from Θ with $L_{\max} = 3$ and $K_{\max} = 64$ for $\mathcal{G}_L$ and $\mathcal{U}_L$ -coded ASP-OFDM as listed in Table I, and from the set of OFDM modulations using K-ary QAM with $K \in \{4, 16, 64\}$ as subcarrier modulation for adaptive OFDM, respectively. Note that the spectral efficiency in Table I can be numerically computed through the power spectral density expressions of the SP-OFDM signals provided in [1] and [4]. Several remarks can be drawn from Figs. 2 and 3. First, all ASP-OFDM signals significantly outperform the adaptive OFDM signals in average spectral efficiency, especially when a higher $\wp$ (inband power fraction) is required. This is primarily due to the fact that the adopted SP-OFDM signals exhibit much higher spectral compactness than the uncoded OFDM signals. Second, the adaptive OFDM schemes with CP perform better in average spectral efficiency than the corresponding adaptive OFDM schemes with ZP. However, a reverse trend is observed for ASP-OFDM. This phenomenon results from the fact that the $\mathcal{G}_L$ and $\mathcal{U}_L$ -coded SP-OFDM

TABLE I
THE CHOSEN Λ OUT OF Θ WITH $L_{\max} = 3$ AND $K_{\max} = 64$ WHEN $N = 8$, $T_g = T_d/8$, $BER_T = 10^{-3}$, AND $\wp = 0.99$ AND 0.999. HERE, λ_v IS REPRESENTED BY THE CORRESPONDING MODULATION PARAMETER PAIR (K, L).

Adaptation Scheme		$\mathcal{G}_L$-coded ASP-OFDM with ZP			$\mathcal{G}_L$-coded ASP-OFDM with CP			$\mathcal{U}_L$-coded ASP-OFDM with ZP			$\mathcal{U}_L$-coded ASP-OFDM with CP		
$\wp$	v	λ_v	Υ_{λ_v}	Φ_{λ_v}	λ_v	Υ_{λ_v}	Φ_{λ_v}	λ_v	Υ_{λ_v}	Φ_{λ_v}	λ_v	Υ_{λ_v}	Φ_{λ_v}
0.99	0	$(4,1)$	7.24	1.39	$(4,1)$	6.94	1.35	$(4,1)$	6.22	1.30	$(4,2)$	6.15	0.95
	1	$(16,1)$	11.46	2.77	$(16,1)$	11.09	2.71	$(16,1)$	10.21	2.59	$(16,2)$	10.19	1.90
	2	$(64,1)$	15.67	4.16	$(64,1)$	15.25	4.06	$(64,1)$	14.23	3.88	$(64,2)$	14.20	2.86
0.999	0	$(4,1)$	7.24	1.22	$(4,1)$	6.94	0.51	$(4,1)$	6.22	0.83	$(4,2)$	6.15	0.65
	1	$(16,1)$	11.46	2.43	$(4,2)$	8.17	0.98	$(16,1)$	10.21	1.66	$(16,2)$	10.19	1.30
	2	$(64,1)$	15.67	3.65	$(16,1)$	11.09	1.02	$(64,1)$	14.23	2.49	$(64,2)$	14.20	1.95
	3	-	-	-	$(16,2)$	12.75	1.95	-	-	-	-	-	-
	4	-	-	-	$(64,2)$	17.32	2.93	-	-	-	-	-	-

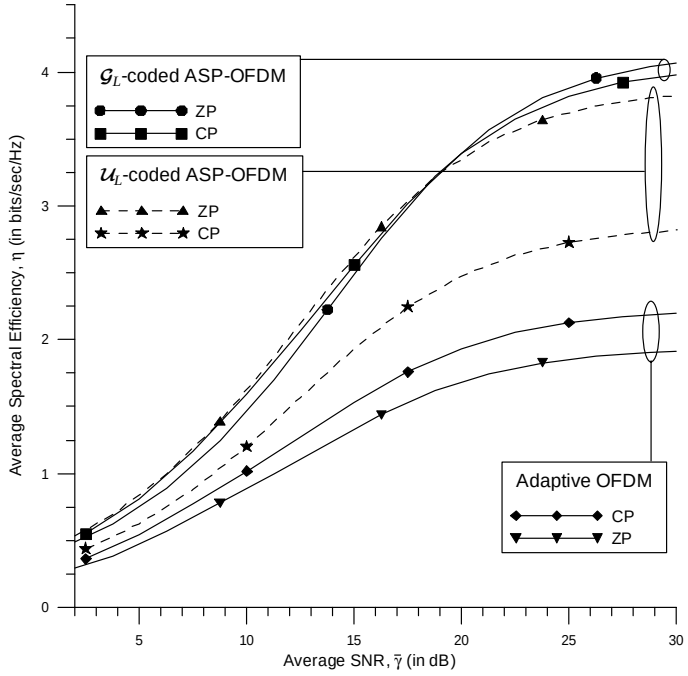

Fig. 2. Average spectral efficiency for ASP-OFDM and adaptive OFDM with $N = 8$, $T_g = T_d/8$, $BER_T = 10^{-3}$, and $\wp = 0.99$.

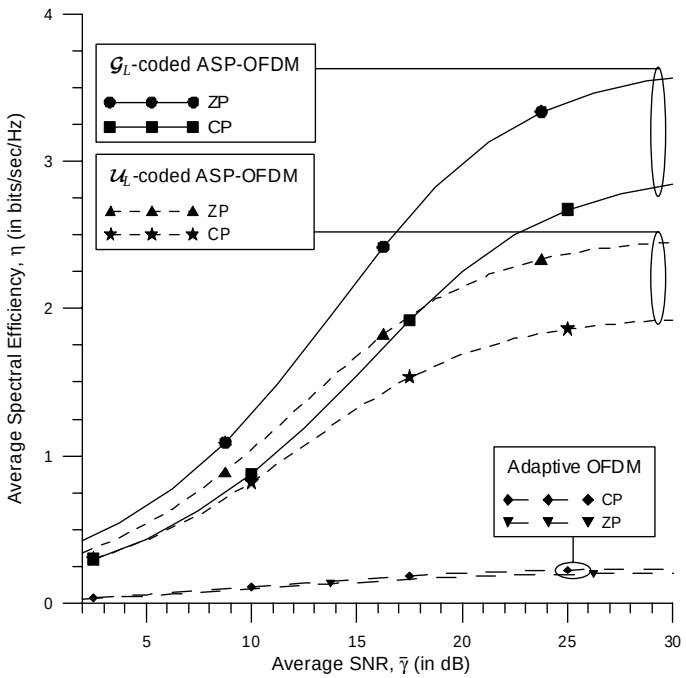

Fig. 3. Average spectral efficiency for ASP-OFDM and adaptive OFDM with $N = 8$, $T_g = T_d/8$, $BER_T = 10^{-3}$, and $\wp = 0.999$.

signals with ZP can provide the power spectral sidelobes decaying asymptotically as f^{-2L-2} with f being the frequency in Hz, and thus outperform in spectral efficiency the $\mathcal{G}_L$ and $\mathcal{U}_L$ -coded SP-OFDM signals with CP which yield the power spectral sidelobes decaying asymptotically as f^{-2} [1]. Finally, when $\wp = 0.999$, $\mathcal{G}_L$-coded ASP-OFDM outperforms $\mathcal{U}_L$-coded ASP-OFDM in average spectral efficiency as shown in Fig. 3. However, $\mathcal{U}_L$-coded ASP-OFDM with ZP scheme performs better in average spectral efficiency than $\mathcal{G}_L$-coded ASP-OFDM with CP and with ZP schemes when $\wp = 0.99$ and the average SNR is low as shown in Fig. 2. The reason results from $\mathcal{U}_L$-coded SP-OFDM with ZP possessing higher spectral compactness when $\wp = 0.99$, but lower spectral compactness when $\wp = 0.999$, than $\mathcal{G}_L$-coded SP-OFDM as also observed in [4].

V. CONCLUSION

The constant-power $\mathcal{U}_L$-coded ASP-OFDM system which adapts the spectral precoder order L and the component modulation size K is studied for the flat fading channels. Due to the extremely high spectral compactness provided by the $\mathcal{U}_L$-coded SP-OFDM signals, $\mathcal{U}_L$-coded ASP-OFDM is found to significantly outperform the conventional adaptive OFDM in average spectral efficiency. Though $\mathcal{U}_L$-coded ASP-OFDM with ZP only performs comparably to $\mathcal{G}_L$-coded ASP-OFDM with CP or ZP when the inband power fraction is 0.99 and the average SNR is not high, $\mathcal{U}_L$-coded ASP-OFDM possesses much lower decoding complexity than $\mathcal{G}_L$-coded ASP-OFDM, which makes $\mathcal{U}_L$-coded ASP-OFDM a more realizable system.

REFERENCES

[1] C.-D. Chung, "Correlatively coded OFDM," *IEEE Trans. Wireless Commun.*, vol. 5, no. 8, pp. 2044–2049, Aug. 2006.

[2] ——, "Spectrally precoded OFDM," *IEEE Trans. Commun.*, vol. 54, no. 12, pp. 2173–2185, Dec. 2006.

[3] ——, "Spectrally precoded OFDM with cyclic prefix," in *Proc. IEEE Int. Conf. Commun.*, pp. 5428–5432, June 2007.

[4] ——, "Spectral precoding for rectangularly-pulsed OFDM," *IEEE Trans. Commun.*, vol. 56, no. 9, pp. 1498–1510, Sept. 2008.

[5] IEEE, *Local and Metropolitan Area Networks Part 16: Air Interface for Fixed Broadband Wireless Access Systems*, IEEE Std. 802.16-2004, Oct. 2004.

[6] M. Faulkner, "The effect of filtering on the performance of OFDM systems," *IEEE Trans. Veh. Technol.*, vol. 49, pp. 1877–1884, Sept. 2000.

[7] W.-L. Lin, C.-D. Chung, and Y.-R. Peng, "Adaptive GL-coded spectrally-precoded OFDM with constant transmission power," in *Proc. IASTED WOC'09*, Banff, Canada, July 6-8, 2009, pp. 105–109.

[8] T. Keller and L. Hanzo, "Adaptive modulation techniques for duplex OFDM transmission," *IEEE Trans. Veh. Technol.*, vol. 49, pp. 1893–1906, Sept. 2000.

[9] B. Choi and L. Hanzo, "Optimum mode-switching-assisted constant-power single- and multicarrier adaptive modulation," *IEEE Trans. Veh. Technol.*, vol. 52, pp. 536–560, May 2003.

[10] S. T. Chung and A. J. Goldsmith, "Degrees of freedom in adaptive modulation: A unified view," *IEEE Trans. Commun.*, vol. 49, pp. 1561–1571, Sept. 2001.